View metadata, citation and similar papers at core.ac.uk
brought to you by CORE
provided by Siberian Federal University Digital Repository

Journal of Siberian Federal University. Biology 2 (2016 9) 198-211
~ ~ ~

УДК 615.46:616.31

Nylon 6, 12/Cloisite 30B Electrospun Nanocomposites for Dental Applications

Snigdha Sajeendra Babu[a], Anju Augustine[a], Nandakumar Kalarikkal[a,b] and Sabu Thomas[a,c]*

[a]International and Inter University Centre for Nanoscience and Nanotechnology, Mahatma Gandhi University Priyadarshini hills P.O., Kottayam 686 560, Kerala, India

[b]School of Pure and Applied Physics, Mahatma Gandhi University Priyadarshini hills P.O., Kottayam 686 560, Kerala, India

[c]School of Chemical Sciences, Mahatma Gandhi University Priyadarshini hills P.O., Kottayam 686 560, Kerala, India

Received 25.12.2015, received in revised form 18.02.2016, accepted 01.05.2016

In this study, nylon-nanoclay fibers were prepared by electrospinning. The electrospun membranes were characterized by fourier transform infra red spectroscopy (FTIR), electron microscopy, X-ray diffraction studies (XRD), contact angle and differential scanning calorimetry (DSC) analyses. The incorporation of nanoclay (Cloisite 30B) to the electrospun membrane which was confirmed by transmission electron microscopy (TEM) showed improvements in the overall properties of the membrane. Antimicrobial studies carried out using Enterococcus faecalis and Candida albicans showed that antimicrobial activity of the membrane with higher clay loading was comparable to that of commercially available dental antiseptic, even though lower clay concentrations did not show antimicrobial effects. The incremental addition of the Cloisite 30B resulted in significant increase in the antimicrobial activity and hydrophobicity.

Keywords: nylon 6,12/clay, composites, electrospun nylon 6,12, dental filler.

DOI: 10.17516/1997-1389-2016-9-2-198-211.

© Siberian Federal University. All rights reserved

* Corresponding author E-mail address: sabuchathukulam@yahoo.co.uk

Полученные методом электростатического формования нанокомпозиты нейлона 6, 12 и клоизита 30B для стоматологического применения

С. Саджендра Бабу[а], А. Августин[а], Н. Каларикал[а,б], С. Томас[а,в]

[а]Международный и национальный университетский центр в области нанонауки и нанотехнологии, Университет им. Махатмы Ганди Индия, штат Керала, г. Коттаям, 686 560 Приядаршини хиллс П.О.

[б]Институт фундаментальной и прикладной физики Университет им. Махатмы Ганди Индия, штат Керала, г. Коттаям, 686 560 Приядаршини хиллс П.О.

[в]Институт химических наук Университет им. Махатмы Ганди Индия, штат Керала, г. Коттаям, 686 560 Приядаршини хиллс П.О.

В работе были получены методом электростатического формования и исследованы волокна композита нейлона и наноглины (клоизит 30B). Мембраны были охарактеризованы с помощью ИК-спектроскопии, рентгеноструктурного анализа, анализа контактных углов и дифференциальной сканирующей калориметрии. Показано, что включение наноглины в мембраны, которое было подтверждено с помощью просвечивающей электронной микроскопии, привело к улучшению свойств мембран. Исследования, выполненные с использованием Enterococcus faecalis и Candida albicans, установили антимикробную активность мембран с высоким содержанием глины, сопоставимую с активностью имеющихся в продаже антисептиков, используемых в стоматологии. В то же время мембраны с низким содержанием глины не проявляли антимикробных свойств. Увеличение содержания клоизита 30B приводило к существенному увеличению антибактериальной активности и гидрофобности мембран.

Ключевые слова: нейлон 6,12 / глина, композиты, электростатическое формование нейлона 6,12, пломбировочный материал.

Introduction

Microbial infections are a major source of concern in materials that find applications in living systems. This requires the scientific community to develop materials that exhibit antimicrobial properties without adversely affecting the biological system and the overall performance of the material. Efforts have been made in this paper

to develop such a filler for use in dental restorative material. Dental amalgams have been used for a long time in dentistry as a restorative material, dental nanocomposites have been preferred ever since the discovery of methacrylate resins about 40 years ago. Methacrylate resins have aesthetic and safety benefits over the dental amalgams. Methacrylate resins have been reinforced with various kinds of fillers to improve the properties of the resulting nanocomposites with properties comparable to that of the dental amalgams (Phillips et al., 1971; Tian et al., 2007), but long term use of the nanocomposites have shown that they are more prone to extensive wear or loss of structural integrity. There is a need for developing a more reliable filler which will help in extending the anatomical integrity over time.

One of the most promising fillers being researched for this purpose are electrospun nylon fibers which have showed improvement in properties of the resulting resins (Tian et al., 2007). Earlier glass fibers, ceramics and whiskers were used as fillers in dental restorative material, which improved the mechanical properties of the resins due to the "bridging" effect caused by their strength and high aspect ratios which reduced the chances of fracture formation (Giordano, 2000). These materials were found to be less effective due to their large size and surface area, which called for the development of nanosized fiberous filler materials with higher aspect ratio and higher surface areas. This will help to increase the resistance to daily wear to which the dental restorative material will be subjected. The addition of nanoclay further enhances the characteristics of the nanofiberous polymeric filler used in the dental restorative material (Usuki et al., 2005) by adding favorable characteristics such as antimicrobial activity (Hong, Rhim, 2008; Wei et al., 2011; Wang et al., 2012) and hydrophobicity, without adversely affecting the living system (Viseras et al., 2009). Nanoclays have the added advantage of being cheap and easily available (Uddin, 2008).

Antimicrobial activity of the filler is essential in order to make sure that the resulting dental restorative material will not harbor any microorganism and thereby alleviating the already existing dental condition. It is known that *Staphylococcus aureus* and *Candida albicans* are prominent bacterial pathogens associated with dental infections (Wei et al., 2011; Wang et al., 2012; Ninan et al., 2014).

This work focuses on studying the properties of one such material showing great potential as a filler for dental nanocomposite. Even though various nylons has been used in some earlier studies (Tian et al., 2007), the addition of nylon 6,12 is preferred in this study due to the properties such as more abrasion resistance and better water repelling property compared to other nylons. An organically modified montmorillonite clay was used as filler for nylon 6, 12. Montmorillonites are layered silicates which are hydrophillic by nature. They are represented by the general formula $(Ca,Na,H)(Al,Mg,Fe,Zn)_2(Si,Al)_4O_{10}(OH)_2XH_2O$. The layer structure contains silicate layers, sandwiching an aluminum oxide/hydroxide layer ($Al_2(OH)_4$) (Uddin, 2008). Organic modification of montmorillonites increases the compatibility of clay to polymeric systems (Singla et al., 2012). Cloisite 30B is the product of organic modification by methyl, tallow, bis-2-hydroxyethyl, quaternary ammonium, where tallow is ~65% C18; ~30% C16; ~5% C14. Cloisite 30B has been shown to impart antimicrobial activity to polymeric materials (Nigmatullin et al., 2009; Parolo et al., 2011; de Azeredo, 2013). The electrospun membranes were studied with different clay loading in order to find an ideal clay loading value.

Electrospinning is a technique used for the electrostatic fiber formation which utilizes

electrical forces to produce polymer fibers with diameters ranging from 2 nm to several micrometres (Augustine et al., 2014). This technique is applicable to all polymer solutions of natural and synthetic origin and this process offers unique capabilities for producing novel nanofibers and fabrics with controllable pore structure (Bhardwaj, Kundu, 2010). The nanofibers produced by electrospinning are of industrial and scientific interest due to their enhanced lengths, small diameters, and high surface area per unit volume. The properties of nanofibers can vary dramatically by different variables that may influence the electrospinning process such as the polymer, solvent, additives, polymer concentration, solution properties, electric field, solution feed rate, nozzle orifice diameter, distance from nozzle to collector, and ambient conditions (Thompson et al., 2007).

Materials and methods

Materials and sample preparation

Nylon (Zytel 151, CAS NO: 26098-55-5) was purchased from Du-Pont, Germany. Clay, Cloisite® 30B was purchased from Rockwood clay additives GmbH, Germany. Formic acid (98%, M = 46.03 g/mol) and dichloromethane (98%, M = 84.93 g/mol) were obtained from Merck specialities private Ltd, India. All materials were used without further purification.

Nylon 6,12 pellets were dissolved in a 1:1 mixture of formic acid (98%) and dichloromethane (98%) by magnetic stirring for 24 h to produce 8 wt% neat nylon solution. Solutions with varying concentrations of cloisite 30B clay were prepared. The clay was added along with nylon pellets at 1 phr, 3 phr, 5 phr and 7 phr concentrations and mechanically stirred for 24 h. The solution was taken in a 20 ml syringe fitted with a 20 gauge blunt needle tip and it was electrospun (Holmark, Model HO-NEV-02) at a high DC voltage of 15 kV, flow rate of 0.8 ml/h. An aluminium sheet of 9 x 7 cm dimension was used as collector. Upon application of uniform force on the syringe, a single droplet is maintained at the tip and on application of high voltage supply a jet of the polymer solution is ejected, which travels towards the grounded collector and on the way the solvent evaporates and polymer fibers are collected on the aluminium sheet. The nonwoven nylon 6, 12 and nylon 6, 12 - nanoclay fibers deposited on the collector were dried in a vacuum oven at room temperature for 12 h before they were characterized.

Electron microscopy

The structural morphology of the electrospun fibers were studied using scanning electron microscopy (SEM-JEOL 6390, Jeol Ltd, Japan). The membrane was carefully section into grids of dimension 3 mm x 0.5 mm and mounted on a SEM grid, the sample was coated with platinum prior to examination. The fiber diameter distribution of the samples were derived using the Image J software, the measurements were made at random positions and the diameter distribution was determined.

The incorporation of layered silicates within the nanofiberous membrane was investigated using transmission electron microscopy (JEOL JEM-2100 HRTEM, Jeol Ltd, Japan). The membrane was cut and placed on a 300 mesh Cu grid (35 mm diameter). The micrographs were obtained in point to point resolution 0.194 nm, operating at an accelerating voltage of 200 kV.

Fourier transform infrared spectroscopy (FTIR)

Fourier transform infrared spectroscopy (Vertex 80v, Bruker Optics) spectra of the samples were measured to verify the types of crystals from 800 to 1600 cm^{-1} with a 4 cm^{-1} resolution. To examine the molecular orientation of the aligned electrospun nanofibers, FTIR equipped with a polarizer was used and the spectra with a 4 cm^{-1}

resolution and the co-addition of 64 scans were recorded.

X-ray diffraction (XRD)

X-ray diffraction (XRD) measurements were performed by Bruker D8 Advance X-Ray Diffractometer using nickel-filtered CuKα radiation operating at 45 kV and 44 mA. All data were collected in the 2θ range of 2 - 40^0 with a scanning rate of 5^0/min.

Differential scanning calorimetry (DSC)

Differential scanning calorimetry was performed by Perkin Elmer Diamond Differential Scanning Calorimeter by heating the sample of 3-4 mg from 20 – 240°C and cooled using liquid nitrogen to 20°C. Heating scans were analyzed for the glass transition temperature, T_g; melting temperature, T_m. The percentage crystallinity of the samples was determined using the enthalpy of fusion using the following equation (Takahashi et al., 2005; Shah et al., 2006):

$$X_c\,(\%) = \Delta H_{expt}/\Delta H_0 * V_f \qquad [1]$$

where, X_c is the percentage of crystallinity, ΔH_{expt} is the enthalpy of fusion of the sample, and ΔH_0 is that of the 100% crystalline standard, and V_f is the volume fraction (Takahashi et al., 2005; Gill et al., 2010).

Contact angle measurements (CA)

Contact angle (CA) measurements were carried out using Contact Analyser, Phoenix 300 (Surface Electro Optics Co. Ltd, Korea). CA of water in air was measured after a water drop was placed on the surface of the membrane using a micro syringe. All membranes were attached on the movable sample platform and levelled horizontally before measurements. The CA on both sides of the drop was measured to check symmetry and horizontal level.

Antimicrobial studies

Enterococcus faecalis and *Candida albicans* cultured for 18 hours were equalized to 0.5 McFarland and swabbed on Mueller-Hinton agar and the surface was allowed to dry for 5 minutes. 50 mg of clay powder was dissolved separately in 1ml DMSO (dimethyl sulphoxide) and sterile distilled water. Stock solution of clay in DMSO, clay in water, 0.2% Chlorhexidine at a concentration of 400 µl/ml were loaded onto Whatman no.1 filter paper discs. Nylon and nylon-nanoclay composite membrane discs of 7 mm were made. Electrospun membrane discs, clay and Chlorhexidine loaded filter paper discs were placed on the agar with the help of sterile forceps and pressed gently. These plates were incubated at 37^0 C overnight. After incubation, zone of inhibition diameter was checked and the antibacterial activity was assessed by measuring the diameter of the zone of inhibition.

Results and discussion

Scanning electron microscopy

From the scanning electron micrographs (Figs. 1-5), it can be noted that the fibers have relatively smooth surface, though the addition of clay to the nylon leads to the formation of ridged fibers, which could have been due to clumping of the fibers. The average fiber diameter of neat nylon 6,12 was 578 nm (Fig. 6). The addition of clay led to a decrease in the fiber diameter, 1 phr clay produced the most drastic decrease in average fiber diameter from 578 nm to 165 nm. The addition of clay maintained the average fiber diameter well below the 300 nm. This can be attributed to the increase in electric conductivity and viscosity of the solution caused by the addition of inorganic clay. The transformation of formed solution droplets into polymer beads upon solvent evaporation is thermodynamically favoured due to the interface reduction. The mutual charge repulsion causes a force directly opposite to the

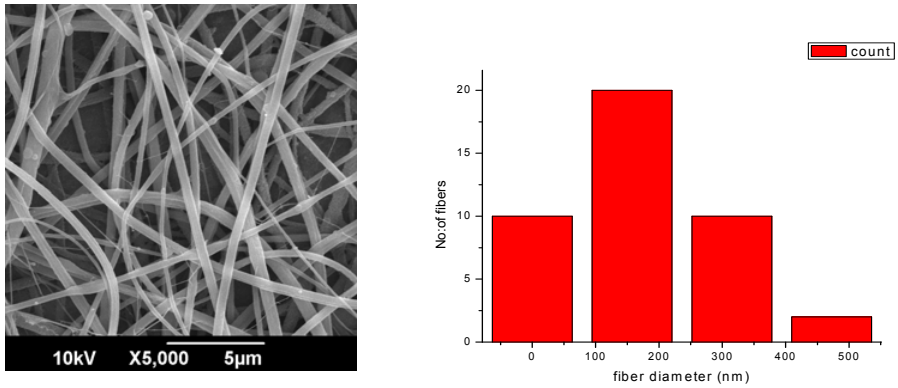

Fig. 1. Scanning electron micrograph (SEM) (left) and fiber diameter distribution (right) of electrospun nylon

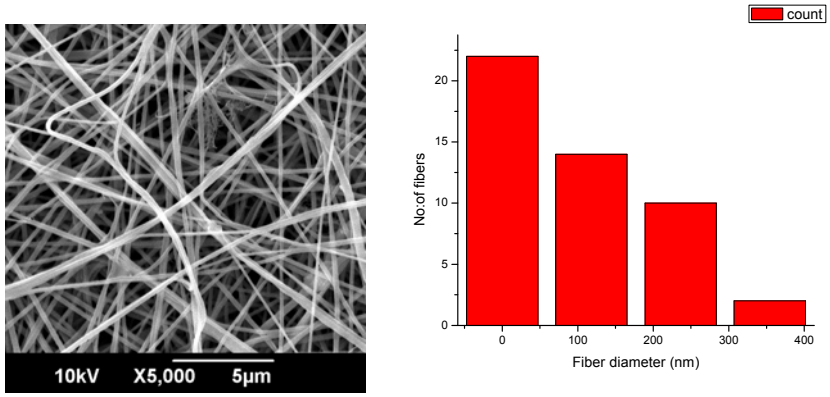

Fig. 2. SEM (left) and fiber diameter distribution (right) of electrospun nylon + 1 phr Cloisite 30B

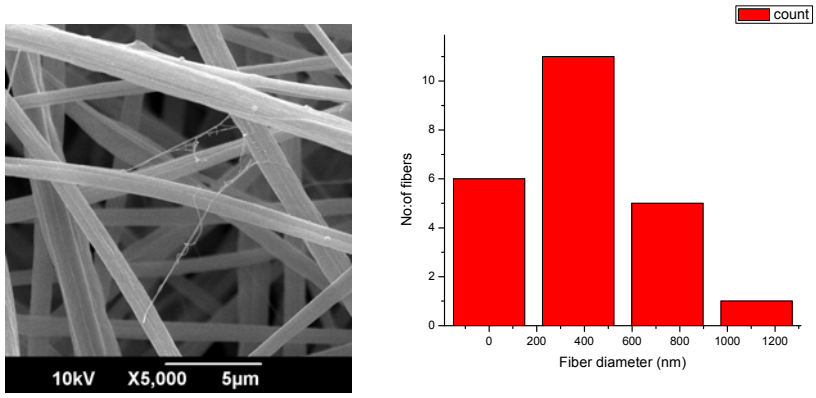

Fig. 3. SEM (left) and fiber diameter distribution (right) of electrospun nylon + 3 phr Cloisite 30B

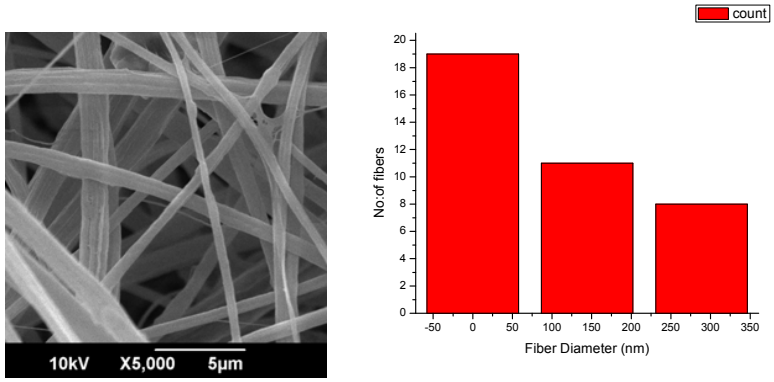

Fig. 4. SEM (left) and fiber diameter distribution (right) of electrospun nylon + 5 phr Cloisite 30B

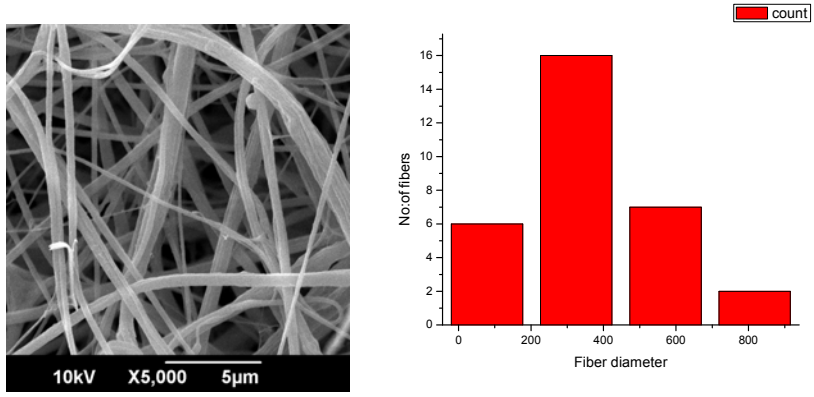

Fig. 5. SEM (left) and fiber diameter distribution (right) of electrospun nylon + 7 phr Cloisite 30B

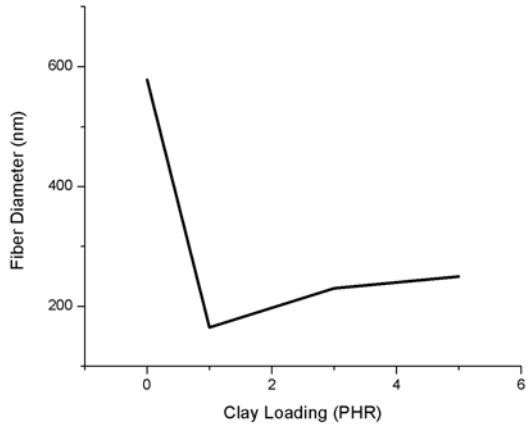

Fig. 6. Average fiber diameter of electrospun nylon fibers with various clay loadings

surface tension and the higher charge density on the surface of the solution jet favours the formation of fine fibers with fewer beads. This is in accordance with the observation of Marras et al. (2008) who demonstrated the production of finer fibrous electrospun nanocomposite material structures upon increasing the clay content (Marras et al., 2008).

It could be observed from figure 6 that the fiber diameter of the electrospun fibers decreased significantly at lower concentration of the clay and the diameter of the fibers increased gradually upon incremental addition of the filler, though the fiber diameters remained significantly lesser than that of the neat nylon fibers.

Transmission electron microscopy

From the TEM images it can be observed that the clay particles have been incorporated into the electrospun nanofibers (Fig. 7). Clay platelets are found to be dispersed in the matrix of nylon 6,12 fibers. Some clay particles were observed in the matrix of the electrospun fibers as well as on the surface.

FTIR analysis

Generally FT-IR is a fundamental tool used to identify the chemical structure and functional groups present in compounds. The chemical interactions between clay and nylon fibers were probed by IR spectroscopy (Fig. 8). The signals characteristic of the neat nylon were observed at 3300 cm^{-1} for N-H stretching, 2900 cm^{-1} for asymmetric CH_2 stretching, 2850 cm^{-1} for symmetric CH_2 stretching, 1639 cm^{-1} for amide stretching, 1539 cm^{-1} for amide II stretching, 1269 cm^{-1} for amide III stretching, 1200 cm^{-1} for symmetric CCH bending and CH2 twisting, 934 cm^{-1} for C-C stretching and 691 cm^{-1} for C-C bending. The Si-AO stretching peaks could be seen at 1086 and 1034 cm^{-1}, Si-AO bending peaks can be seen at 520 and 467 cm^{-1}, these are characteristic of Cloisite 30B (Mohanty et al., 2012). Thus the IR spectrum of nanocomposites confirms the presence of all functional groups on nylon and clay in the composite samples. There are no significant changes in the FTIR spectrum of the nanocomposite when compared to neat nylon; this indicates that there is no significant chemical interaction between nylon and nanoclay.

X-ray diffraction studies

Fig. 9 shows the X- ray diffraction patterns of nylon 6, 12, clay, and nylon 6, 12 - clay nanocomposites at 1 phr, 3 phr, 5 phr and 7phr. The nylon shows multi crystalline forms (i.e.

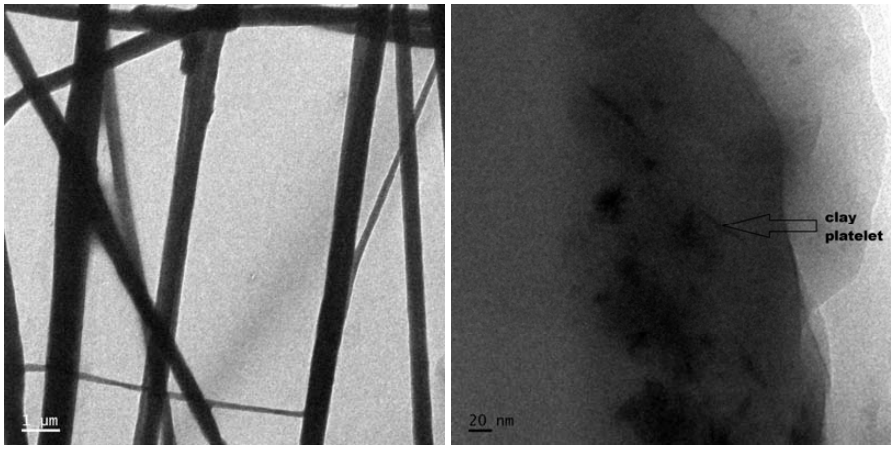

Fig. 7. HRTEM images of electrospun nylon-clay membrane (1 phr) at different magnifications.

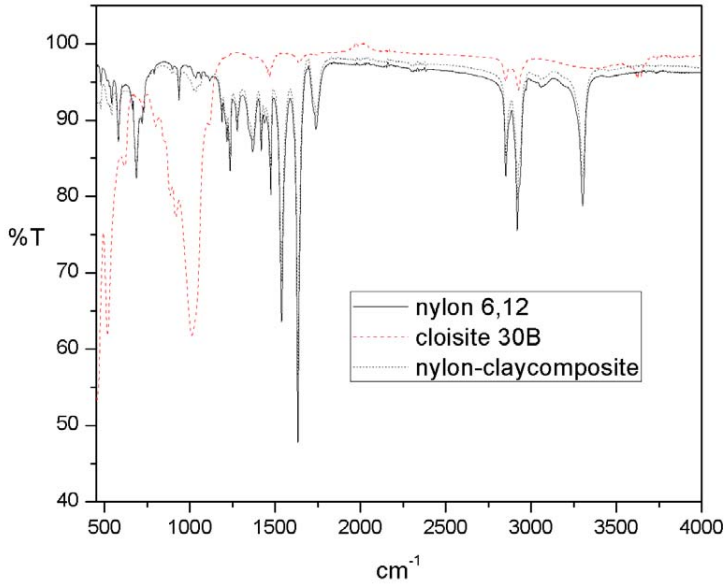

Fig. 8. FTIR of nylon, Cloisite 30B, and nylon-clay composite

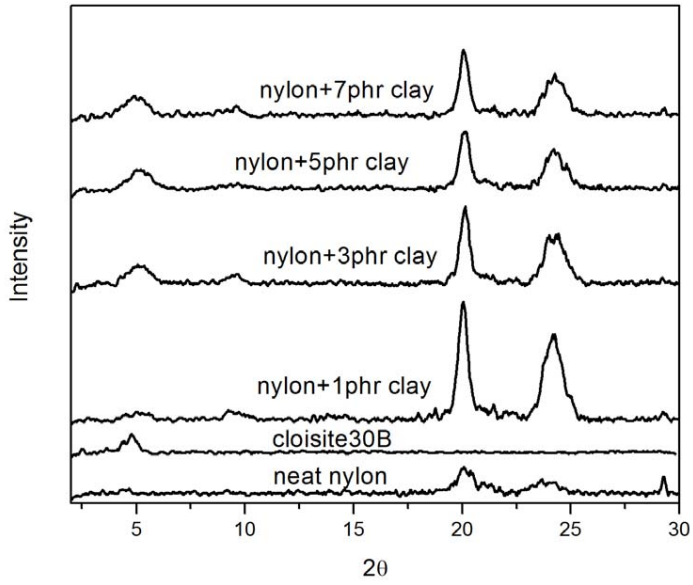

Fig. 9. XRD profiles of nylon, Cloisite 30B, and nylon – clay nanocomposites

polymorphism) and usually exhibit a more stable α crystalline form rather than the β and γ crystalline forms. The neat polymer shows two α crystalline peaks respectively at $2\theta = 20^0$ and 25^0 and pure clay shows a peak at $2\theta = 5^0$. At 1 phr concentration, the intensity of the peaks at $2\theta = 5^0$ is decreased, whereas the peaks at $2\theta = 20^0$ and 25^0 have increased significantly showing an increase in crystallinity of the polymer matrix. The reasons for this phenomenon are not clearly known but it assumed that the increase in crystallization is due to the

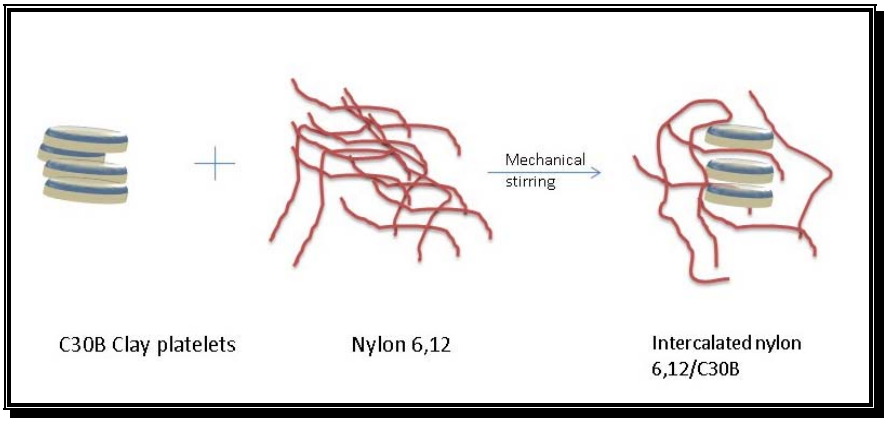

Fig. 10. Intercalation between the nylon polymer chains and aluminosilicate platelets at 1 phr clay concentration

interaction between the polymer chains and aluminosilicate platelets (Fig. 10). This interaction may cause better alignment of the nylon fibers. The decrease in intensity of the clay peaks indicates the diffusion of polymer chains into the clay galleries, thus expanding the clay structure. It could be inferred that the morphology of the nanocomposite is mainly intercalated at 1 phr clay loading and there is good interaction between the polymer and filler (Liu, Breen, 2005; Li et al., 2006). But upon increasing the clay content, there is a decrease in the intercalation of clay in the polymer matrix, observed by the increase in intensity of the clay peaks and a corresponding decrease in the intensity of the nylon peaks. This indicates that the clay probably plays an important role in increasing the crystallization rate of the nylon at a lower filler concentration by acting as nucleating agents (Huang et al., 2014).

Differential scanning calorimetry

Differential scanning calorimetry of the electrospun membrane was studied to see the effect of clay loading the degree of crystallization. It can be seen (Table 1) that there is an increase in the percentage crystallinity with the addition of nanoclay to nylon 6,12 and then with increasing concentration of Cloisite 30 B the crystallinity is found to be decreasing; this could be because clay particles serve as additional nucleation sites, but on higher clay loading the nucleation process is slowed down. At low clay concentrations, the particles are highly dispersed and there is a possibility of incorporating additional nucleation sites, but higher clay concentrations hinder the diffusion of polymer chain into the growing crystallite (Fornes, Paul, 2003). There is a significant shift in the glass transition temperature T_g, indicating immobilisation of the polymer chains upon increasing the clay concentration in the matrix.

Contact angle measurements

From the contact angle studies (Fig. 11, Table 2), it is clear that the addition of nanoclay to the nylon membrane tends to augment the hydrophobicity of the electrospun membrane. Upon addition of small increments of nanoclay, the hydrophobicity of the membrane also increased slightly. The hydrophobicity is a desirable property for dental restorative material. In this experiment, Cloisite 30B has been used which is organically modified

Table 1. Differential scanning calorimetry results for electrospun membranes

Composition	% Crystallinity	Melting Temperature (T_m)	Glass Transition Temperature (T_g)
Neat nylon	24.7	223.0	40.1
Nylon + 1 phr Clay	31.0	230.7	44.8
Nylon + 3 phr Clay	31.7	230.0	47.0
Nylon + 5 phr Clay	28.5	226.0	47.6
Nylon + 7 phr Clay	22.6	229.0	50.6

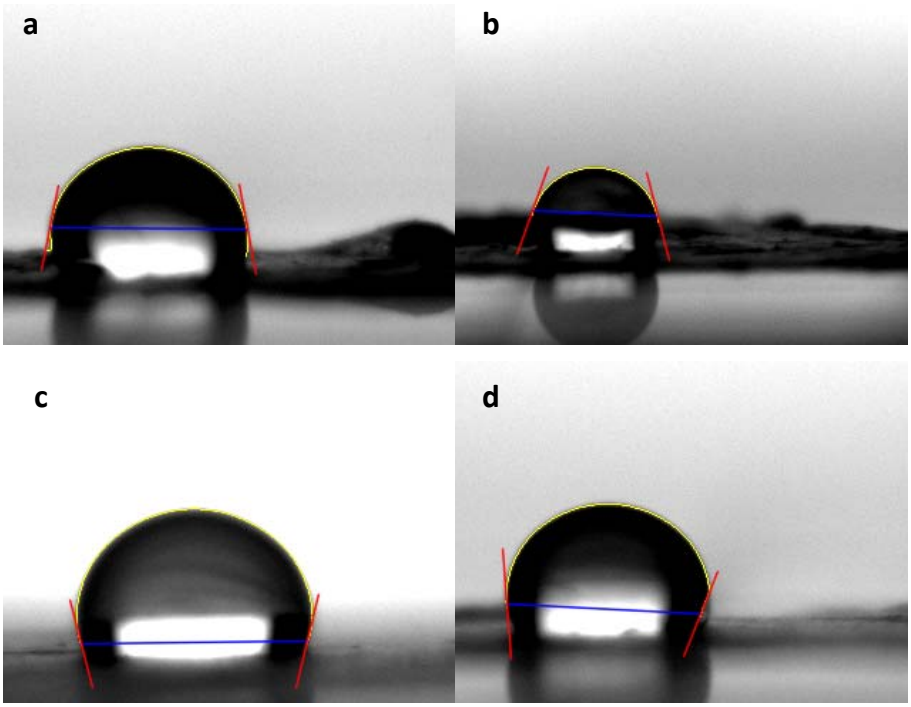

Fig. 11. Contact angle of water droplets on (a) Neat nylon electrospun membrane; (b) Nylon-nanoclay composite membrane 0.1 wt%; (c) Nylon- nanoclay composite membrane 0.5 wt%; (d) Nylon-nanoclay composite membrane 1 wt%

Table 2. Water contact angle values for the electrospun composite membranes

Concentration of nanoclay in nylon (wt%)	Contact Angle (°)
0.0	95
0.1	97
0.5	99
1.0	103

montmorillonite. Organic modification increases the hydrophobicity of the nanoclay thus making it easier for it to be miscible with non-polar polymers. This explains the increase in contact angle of the nylon/nanoclay membranes upon addition of the organically modified nanoclay (Lin et al., 2010).

Antimicrobial activity

Fig. 12 represents the antimicrobial studies carried out with *E. fecalis* and *C. albicans* which are common pathogens invading the oral cavity. It is clear that the electrospun nylon membrane has no activity on the microorganisms, but on increasing the concentration of nanoclay in the electrospun membrane, a clear zone of growth inhibition could be seen around the membranes with higher clay loading. Clay loaded sterile filter paper discs were also used in the test. These discs show significant antimicrobial activity comparable to that of the commercially available dental antiseptic (clorhexidine). This significant antimicrobial activity can be attributed the large surface area and the ionic charged surface of the organically modified clay platelets which tend to attract polar surfaces. Since the bacterial membranes are charged they are attracted to the clay platelets and the platelets tend to block essential membrane functions (Wei et al., 2011; Wang et al., 2012).

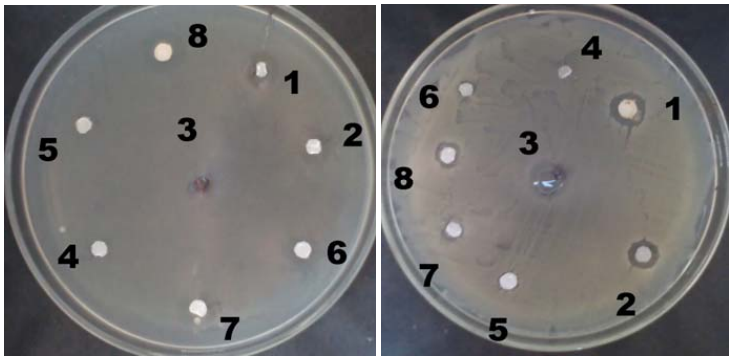

Fig. 12. Antimicrobial activity of electrospun membranes against *E. fecalis* (left) and *C. albicans* (right). 1. Clay in DMSO; 2. Clay in H_2O; 3. 0.2 % Chlorhexidine; 4. Pure nylon; 5. Nylon + 1 phr clay; 6. Nylon + 3 phr clay; 7. Nylon + 5 phr clay; 8. Nylon + 7 phr clay

Table 3. Antimicrobial activity of electrospun membranes against *Enterococcus fecalis* and *Candida albicans*

Nº	Samples	Diameter of inhibition zone (mm)	
		E. fecalis	*C. albicans*
1	Clay in DMSO	16.0	16.0
2	Clay in H_2O	14.0	11.0
3	0.2 % Chlorhexidine	13.0	12.0
4	Pure nylon	0	0
5	Nylon + 1 phr clay	0	0
6	Nylon + 3 phr clay	10.0	0
7	Nylon + 5 phr clay	10.5	9.0
8	Nylon + 7 phr clay	15.0	10.0

Conclusion

In this study, the preparation and various analyses of nylon-nanoclay fibers were discussed. The electrospun nylon 6,12/nanoclay nanocomposite showed marked improvements in the properties when compared to nylon membrane. SEM micrographs show a decrease in fiber diameter upon the addition of clay and TEM shows the successful incorporation of nanoclay in the nylon fibers. Desirable properties such as excellent antimicrobial activity as well as hydrophobicity were shown by membranes with higher clay loading. The increase in crystallinity followed by decrease in crystallinity upon increasing the clay loading was observed in the XRD and DSC, which indicates a higher level of interaction at lower clay loadings. The T_g shift to higher temperatures at higher clay loadings also indicates that nylon 6,12/nanoclay nanocomposite can prove to be very good candidate as filler in dental resins. These nanocomposite fibers with improved properties can be added to BisGMA/TEGDMA dental resins to obtain improved dental fillers with enhanced aesthetic, antibiotic and physical properties.

Acknowledgement

The authors would like to thank Indian Council of Medical Research (ICMR, India) for funding this project and the instrument facilities at International and Inter University Centre for Nanoscience and Nanotechnology and Mahatma Gandhi University.

References

Augustine R., Malik H.N., Singhal D.K., Mukherjee A., Malakar D., Kalarikkal N., Thomas S. (2014) Electrospun polycaprolactone/ZnO nanocomposite membranes as biomaterials with antibacterial and cell adhesion properties. *J Polym Res*, 21(3): 1-17

Bhardwaj N., Kundu S.C. (2010) Electrospinning: a fascinating fiber fabrication technique. *Biotechnol Adv*, 28(3): 325-347

de Azeredo H. (2013) Antimicrobial nanostructures in food packaging. *Trends in Food Science & Technology*, 30(1): 56-69

Fornes T., Paul D. (2003) Crystallization behavior of nylon 6 nanocomposites. *Polymer*, 44(14): 3945-3961

Gill P., Moghadam T.T., Ranjbar B. (2010) Differential scanning calorimetry techniques: applications in biology and nanoscience. *Journal of biomolecular techniques: JBT*, 21(4): 167-193

Giordano R., 2nd (2000) Issues in handling impression materials. *Gen Dent*, 48(6): 646-648

Hong S.I., Rhim J.W. (2008) Antimicrobial activity of organically modified nano-clays. *J Nanosci Nanotechnol*, 8(11): 5818-5824

Huang Y., Miao Y.E., Ji S., Tjiu W.W., Liu T. (2014) Electrospun carbon nanofibers decorated with ag-pt bimetallic nanoparticles for selective detection of dopamine. *ACS Appl Mater Interfaces*, 6(15): 12449-12456

Li L., Bellan L.M., Craighead H.G., Frey M.W. (2006) Formation and properties of nylon-6 and nylon-6/montmorillonite composite nanofibers. *Polymer*, 47(17): 6208-6217

Lin J.J., Chan Y.N., Lan Y.F. (2010) Hydrophobic modification of layered clays and compatibility for epoxy nanocomposites. *Materials*, 3(4): 2588-2605

Liu X., Breen C. (2005) High-temperature crystalline phases in nylon 6/clay nanocomposites. *Macromolecular rapid communications*, 26(13): 1081-1086

Marras S.I., Kladi K.P., Tsivintzelis I., Zuburtikudis I., Panayiotou C. (2008) Biodegradable polymer nanocomposites: the role of nanoclays on the thermomechanical characteristics and the electrospun fibrous structure. *Acta Biomater*, 4(3): 756-765

Mohanty D.P., Palve Y.P., Sahoo D., Nayak P. (2012) Synthesis and characterization of chitosan/ cloisite 30B (MMT) nanocomposite for controlled release of anticancer drug curcumin. *International Journal of Pharmaceutical Research & Allied Sciences*, 1(4): 52-62

Nigmatullin R., Gao F., Konovalova V. (2009) Permanent, non-leaching antimicrobial polyamide nanocomposites based on organoclays modified with a cationic polymer. *Macromolecular Materials and Engineering*, 294(11): 795-805

Ninan N., Muthiah M., Bt Yahaya N.A., Park I.K., Elain A., Wong T.W., Thomas S., Grohens Y. (2014) Antibacterial and wound healing analysis of gelatin/zeolite scaffolds. *Colloids and Surfaces B: Biointerfaces*, 115: 244-252

Parolo M., Fernández L., Zajonkovsky I., Sánchez M., Bastion M. (2011) Antibacterial activity of materials synthesized from clay minerals. *Science against microbial pathogens: communicating current research and technological advances. Formatex, Microbiology series*, (3): 144-151

Phillips R.W., Avery D.R., Mehra R., Swartz M.L., McCune R.J. (1971) One-year observations on a composite resin for Class II restorations. *J Prosthet Dent*, 26(1): 68-77

Shah B., Kakumanu V.K., Bansal A.K. (2006) Analytical techniques for quantification of amorphous/crystalline phases in pharmaceutical solids. *Journal of pharmaceutical sciences*, 95(8): 1641-1665

Singla P., Mehta R., Upadhyay S.N. (2012) Clay modification by the use of organic cations. *Green and Sustainable Chemistry*, 2: 21-25

Takahashi H., Chen R., Okamoto H., Danjo K. (2005) Acetaminophen particle design using chitosan and a spray-drying technique. *Chemical and pharmaceutical bulletin*, 53(1): 37-41

Thompson C.J., Chase G.G., Yarin A.L., Reneker D.H. (2007) Effects of parameters on nanofiber diameter determined from electrospinning model. *Polymer*, 48: 6913-6922

Tian M., Gao Y., Liu Y., Liao Y., Xu R., Hedin N.E., Fong H. (2007) Bis-GMA/TEGDMA dental composites reinforced with electrospun nylon 6 nanocomposite nanofibers containing highly aligned fibrillar silicate single crystals. *Polymer*, 48(9): 2720-2728

Uddin F. (2008) Clays, nanoclays, and montmorillonite minerals. *Metallurgical and Materials Transactions A*, 39(12): 2804-2814

Usuki A., Hasegawa N., Kato M., Kobayashi S. (2005) Polymer-clay nanocomposites. *Inorganic Polymeric Nanocomposites and Membranes*. Springer, p. 135-195

Viseras M.T., Aguzzi C., Cerezo P., Cultrone G., Viseras C. (2009) Supramolecular structure of 5-aminosalycilic acid/halloysite composites. *J Microencapsul*, 26(3): 279-286

Wang M.C., Lin J.J., Tseng H.J., Hsu S.H. (2012) Characterization, antimicrobial activities, and biocompatibility of organically modified clays and their nanocomposites with polyurethane. *ACS Appl Mater Interfaces*, 4(1): 338-350

Wei J.C., Yen Y.T., Su H.L., Lin J.J. (2011) Inhibition of bacterial growth by the exfoliated clays and observation of physical capturing mechanism. *The Journal of Physical Chemistry C*, 115(38): 18770-18775